Well-Defined Oxide Core-Poly(vinyl pyrrolidone) Shell Nanoparticles: Interactions and Multi-Modal Glass Transition Dynamics at Interfaces

Vladimir Bershtein,[*1] *Vladimir Gun'ko,*[2] *Larisa Egorova,*[1] *Natalia Guzenko,*[2] *Eugene Pakhlov,*[2] *Valery Ryzhov,*[1] *Vladimir Zarko*[2]

Summary: Interfacial interactions and dynamics were studied in silica and alumina core-poly(vinyl pyrrolidone) (PVP) shell nanoparticles with different shell thicknesses starting from 1-2 nm (monolayer); their geometry and structural organization were comprehensively characterized by several techniques. Far- and mid-IR spectroscopy, combined with DSC activation analysis of the glass transition, allowed to register hydrogen bonding and Lewis/Brønsted interactions, and the multi-modal glass transition dynamics in PVP nanoshells, as well as their interrelationship. For PVP monolayer, only a few ''abnormal'' modes constituted glass transition which covered the temperature range from 80 to 230 °C, with varying the activation energy by an order of magnitude.

Keywords: calorimetry; core-shell nanoparticles; glass transition; infrared spectroscopy; interfaces

Introduction

Due to enormous interfacial area, polymer nanocomposites may be considered to a large extent as the ''interface-controlled'' materials. Starting from the works,[1–4] a large series of the experimental studies of dynamics for polymers in ultrathin films, adsorbed on solid substrates or in free-standing state, and in nanovolumes of polymer nanocomposites have been performed and reviewed in.[5–7] As shown, glass transition characteristics may dramatically differ from those in a bulk polymer (in particular in polymer-silica nanocomposites,[8–10]) with slowing down or acceleration of dynamics, under these conditions due to constrained dynamics/nanoconfinement effects or at free surface.

Nevertheless, much experimental research still remains to be done in order to trace the connections between interfacial interactions and peculiar polymer dynamics, especially within the interfacial 1-2 nm thick monomolecular polymer layers. This is of importance for the development of high performance polymer nanocomposites, adhesives, coatings and core-shell nanoparticles for technical, medical and other applications.

Previously,[11–14] the oxide core- poly-(vinyl pyrrolidone) (PVP) shell nanoparticles have been prepared and characterized by different techniques. Recently, far- and mid-IR spectra revealed two kinds of strong PVP-silica interactions, maximal for 1-2 nm thick monomolecular PVP shell: hydrogen bonding and, tentatively, ''soft'' Lewis acid-base interactions; this resulted in a complicated dynamics in the PVP glass transition.[14]

In this paper, we report some results of the comparative analysis of the interrelationship between interfacial interactions, as studied by IR spectroscopy, and glass

[1] Ioffe Physical -Technical Institute, Russian Academy of Sciences, 26 Politechnicheskaya str, St.-Petersburg 194021, Russia
Fax: (+7) 812 2971017;
E-mail: vbersht@polmater.ioffe.ru
[2] Institute of Surface Chemistry, National Academy of Sciences of Ukraine, 17 General Naumov str, Kiev 03164, Ukraine

Copyright © 2010 WILEY-VCH Verlag GmbH & Co. KGaA, Weinheim

transition dynamics at interfaces estimated by DSC, in well-defined silica core-PVP shell and alumina core-PVP shell nanoparticles. The measurements were performed for interfacial PVP monomolecular layer and the thicker PVP nanoshells, that is, when varying the impact of interfaces to segmental dynamics. In previous work[14] and this paper for the first time far-IR spectroscopy combined with DSC analysis of the dispersion of activation barriers to dynamics in the glass transition were applied to studying polymer nanolayers.

Core-Shell Particles Characterization

The oxide/PVP nanoparticles with different weight compositions were prepared, as previously,[11–14] in a pseudo-liquid state reactor (PLSR). This procedure provided a maximal amount of PVP-oxide contacts and uniform distribution of PVP on oxide surface, in contrast to poor polymer distribution in the initial PVP/oxide mixtures (see below). Core-shell particles obtained were characterized by combined utilizing low-temperature nitrogen adsorption (LTNA), quasi-elastic light scattering (QELS), atomic force microscopy (AFM), FT-IR spectroscopy and densitometry techniques.[14]

Fumed 3D silica and alumina nanoparticles with 6–16 nm (on average 9 nm) or 10–50 nm (on average 25 nm) size, respectively, and with specific surface areas $S_{BET} = 342\ m^2/g$ (SiO_2) and $79\ m^2/g$ (Al_2O_3) (LTNA), as well as commercial PVP with $M_n = 12600 \pm 2700$ g/mol were used. At PVP content $C_{PVP} = 20$ or 40 wt%, primary core-shell nanoparticles formed secondary highly-porous aggregates with ~100-800 nm size after the treatment in the pseudo-liquid state (AFM, QELS); their pore radius varied from 0.3 to 100 nm (LTNA), and bulk density ρ_b was ~ 0.1–0.3 g/cm^3. With increasing PVP content to 80–90 wt%, practically non-porous, high-density nanocomposite structures were formed.

The LTNA/QELS/density analysis data were used for the calculation of the PVP shell thickness, h_{PVP}, as a function of PVP content in the samples (Figure 1). Shell thicknesses were estimated for two boundary cases: (*i*) individual primary oxide nanoparticles covered by PVP, and (ii) PVP-covered aggregates of these nanoparticles. For the samples with 20 or 40 wt% PVP, the shell thickness was, obviously, more close to the lower boundary whereas at $C_{PVP} = 80$ or 90 wt% PVP the thickness of a polymer layer between individual oxide nanoparticles increased by a factor of two due to compacting PVP-covered oxide particles, and it was more close to the upper boundary.

Figure 1 shows that the thickness h_{PVP} varied, depending on PVP content, from 1–2 to 20–100 nm. Taking into account that radius of gyration for PVP macromolecules with $M_n = 12600$ g/mol and about 25 nm in length equals $R_g \approx 8$ nm, and strongly adsorbed chains acquire the flattened quasi-2D conformations,[15,16] practically monomolecular PVP layers were present on oxide surface in the 20PVP/80SiO_2, 20PVP/80Al_2O_3 and 40PVP/60SiO_2 particles.

Interfacial Interactions and Dynamics

Interfacial interactions in the PVP-oxide nanoparticles may be controlled, besides the dispersion forces, by strong hydrogen

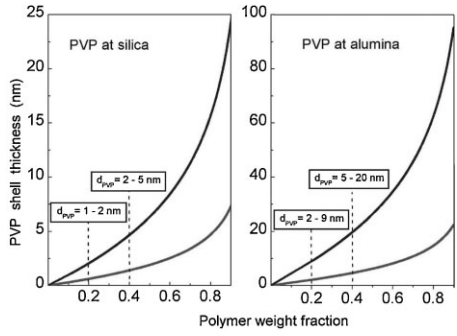

Figure 1.
PVP shell thickness as a function of polymer fraction in PVP/SiO_2 and PVP/Al_2O_3 nanoparticles. The lower curves relate to uniform PVP shell of individual oxide nanoparticles, and the upper ones relate to PVP layers in particle aggregates (LTNA/QELS/density analysis).

Copyright © 2010 WILEY-VCH Verlag GmbH & Co. KGaA, Weinheim

bonding and, presumably, ''soft'' Lewis-Brønsted (LB) acid-base interactions. According to quantum chemical calculations, the energy of H-bonds between NC=O and Si–OH groups of silica surface equals 40–50 kJ/mol whereas the interaction energy between PVP molecules equals only 7 kJ/mol.[13] This difference determines the preferable adsorption of PVP molecules onto uncovered oxide surface after treatment of powdered PVP/oxide mixture in the PLSR, due to increased mobility and migration macromolecules to uncovered oxide surface with formation of a relatively uniform polymer nanoshell. Monomolecular PVP shell of oxide nanoparticles (at $C_{PVP} = 20$ wt%) could not be washed off due to the irreversible adsorption.

The LB interactions between polar polymers and oxides are discussed.[17–19] PVP is considered as a rather strong Lewis base,[19,20] and its LB interaction with amorphous fumed silica particles, obtained under ultrahigh-temperature conditions, are possible due the presence of twin silanols with the enhanced acidity and the active silicon atoms as electron deficient Lewis centers at silica surface.[21] However, the quantum chemical investigations showed that the hydrogen bonding between PVP and silica surface is preferable.[13]

The stronger LB interactions may be expected, however, for the adsorption of PVP at fumed alumina surface. According to our X-ray analysis, alumina particles have crystalline γ-phase structure possessing incompletely O-coordinated Al atoms as the Lewis acid sites and $(\equiv AlO)_2H$ as weak Brønsted centers. Secondly, alumina is a well known catalyst in acid/base reactions occurring at these centers.[22] And, thirdly, we performed the experiments on adsorption of the electron-donor Dimethylaminoazobenzene (DMAAB) as a color (Hammett) indicator to study the active LB centers on fumed silica and alumina surfaces by means of optical spectroscopy (in the region of 490–560 nm). The spectra obtained confirmed much more presence of L-and B-centers at alumina surface than at silica surface.

Some contribution to interfacial interactions in the systems under study is provided by sorbed water despite the special measures to obtain dry samples for IR measurements.[14] PVP-H_2O complexes with H-bond enthalpy of 25 kJ/mol are formed,[23] and some water re-adsorption at oxide surface occurred during preparing samples after thermal treatment. Nevertheless, water adsorbed onto oxides forms cluster structures, and a significant part of the oxide surface remains free from adsorbed water.[24] Additionally, water is replaced to large extent by PVP during PLSR treatment due to much stronger NC=O/oxide interactions. Water was totally removed in the DSC experiments.

The FT-IR spectra (ThermoNicoler FT-IR spectrometer) of uncovered silica show the presence of free silanol groups ($\sim 3740\,cm^{-1}$) as the potential centers for the hydrogen bonding with PVP even in the presence of adsorbed water ($3200–3500\,cm^{-1}$); after dehydration at 473 K their concentration increases (Figure 2, a). Such centers are much less pronounced at the alumina surface; water desorption occurs only partly at 473 K in this case (Figure 2, b). Therefore, the lesser role of the interfacial hydrogen bonds might be presumed for the PVP/Al_2O_3 nanoparticles.

Figure 3 shows that the FT-IR spectrum of relatively dry 20PVP/80SiO_2 mixtures is akin to that of the neat fumed silica (the intense band $3730–3750\,cm^{-1}$ that evidences poor PVP distribution on the silica surface.[11] After PLSR treatment, the PVP distribution on silica surface cardinally changes: swelling of PVP leads to increasing segmental mobility and migration of molecules onto silica surface places free of PVP. This rearrangement forms relatively uniform nanoshell. Really, practically all free silanols on silica surface disappear already after adsorption of 20 wt% PVP (monolayer), due to the interaction with PVP (Figure 3). Disappearance of the $3730–3750\,cm^{-1}$ band was observed also for the thicker PVP shells.

To characterize interfacial interactions, the peculiarities of molecular dynamics and conformational state in PVP shells compared with those in bulk PVP, far-IR

Copyright © 2010 WILEY-VCH Verlag GmbH & Co. KGaA, Weinheim

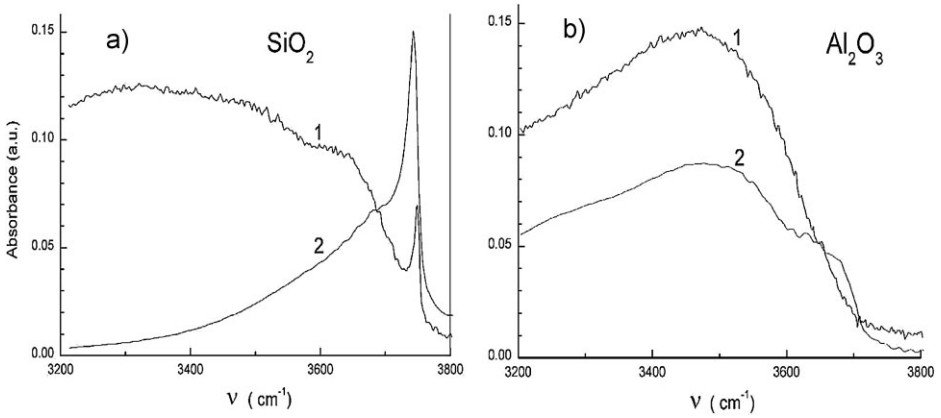

Figure 2.
FT-IR spectra of uncovered silica and alumina nanoparticles (pressing in KBr tablets) in the region of the absorption bands of surface OH groups and adsorbed water at 293 K (1) and 473 K (2).

spectra at 20–500 cm^{-1} were registered using FIS-21 Hitachi spectrometer. Low-density polyethylene (LDPE) matrix as the transparent medium in this spectral region, which besides isolated samples from atmospheric water, was used. The sample/LDPE powder mixtures (1:100) were prepared with thermal drying treatments, and monolithic films with 100–300 μm in thickness were prepared as described elsewhere.[14]

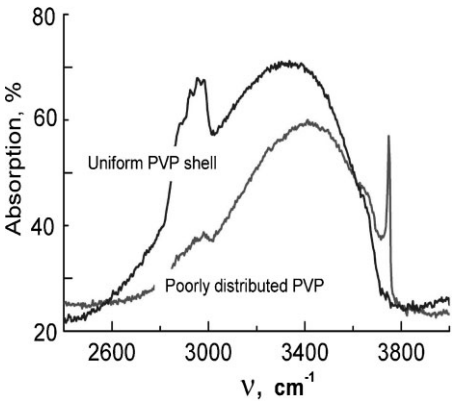

Figure 3.
FT-IR spectra of "dried" 20PVP/80SiO_2 nanoparticles (pressing in KBr tablets) in the region of the absorption bands of SiOH groups and sorbed water before and after exposition powdered mixtures in saturated vapour of water/ethanol mixture (1:1) (pseudo-liquid state), that is, with poor distribution of PVP at silica surface and its uniform distribution with formation of uniform PVP shell, respectively.

To obtain the spectra of neat PVP and PVP shells, the reference spectra of neat LDPE and LDPE/neat silica films with the same effective thicknesses of silica and LDPE as in the studied films were also obtained. Three repeat measurements were performed in all cases. The absorption coefficients $k = d_{\text{eff}}^{-1} \ln(I_0/I)$ were determined where d_{eff} is the effective thickness of PVP layer estimated from the sample composition; I is the transmission of a studied film, and I_0 is the transmission of a reference film (LDPE or LDPE/silica).

The far-IR spectra, obtained for neat PVP and PVP shells with ~1-2 nm thickness (monomolecular layer, the 20PVP/80SiO_2, 40PVP/60SiO_2, 20PVP/80Al_2O_3 samples) and the thicker nanoshellls (Figure 1), are presented in Figure 4. Seven partly overlapping absorption bands with the maxima at 42, 83, 100, 169, 247, 355 and 446 cm^{-1} can be seen in the far-IR spectrum of neat PVP. The assignments of these bands observed in the spectra of PVP and PVP nanoshells are given in Table 1. The relative values of absorption coefficients for the absorption bands characterizing the interfacial interactions are given in Table 2.

These data demonstrate the substantial changes in the PVP far-IR spectrum when PVP was transformed into nano-dispersive adsorbed state, i.e., for monomolecular 1–2 nm and the thicker PVP nanoshells. These

Copyright © 2010 WILEY-VCH Verlag GmbH & Co. KGaA, Weinheim

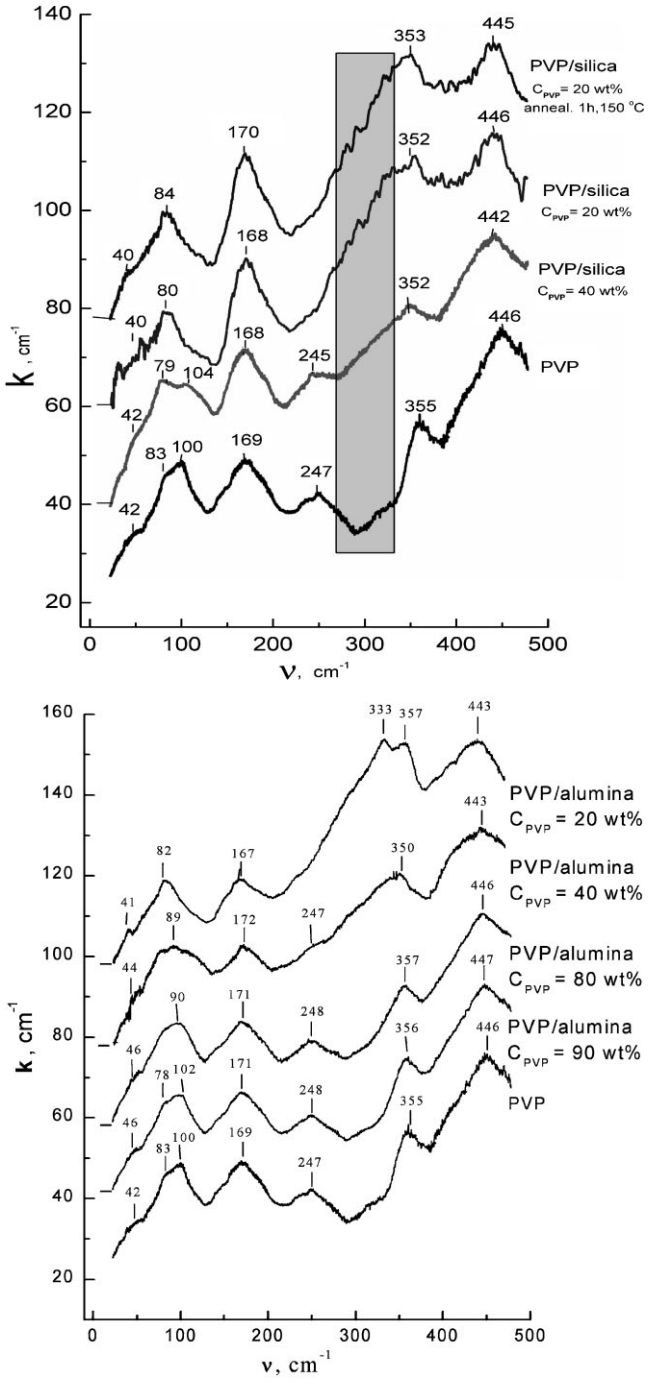

Figure 4.
Far-infrared spectra of neat PVP and PVP shells in the PVP/oxide nanoparticles with different content C_{PVP} and shell thickness (see Figure 1). The spectra of PVP shells are shifted along the ordinate axis relative to the spectra of neat PVP.

Copyright © 2010 WILEY-VCH Verlag GmbH & Co. KGaA, Weinheim

Table 1.
Absorption bands in the far-IR spectra of PVP in bulky state and nanoshells1.[14,25]

Absorption band (cm^{-1})	Assignment
40–46	Hydrogen bonds, torsional vibrations[a)]
78–104	Small-angle pyrrolidone ring vibrations (librations), Poley-type absorption
167–172	Hydrogen bonds, stretching vibrations[a)]
245–248	Torsional skeletal vibrations
~ 250 to 350	PVP/oxide Lewis/Brønsted interactions[b)]
350–357	Deformation pyrrolidone ring vibrations
442–447	Ditto

[a)]H-bonds in neat PVP were assigned to PVP-residual water complexes.
[b)]Tentative assignment (see text).

changes relate to interfacial interactions, and to dynamics and conformational state of chains at the interfaces; they are most pronounced for PVP monolayers ($C_{PVP} = 20$ wt%). Additionally, the substantial difference in the spectra of PVP nanolayers of similar thicknesses, adsorbed at silica and alumina surfaces, are also observed.

Generally, four peculiarities of the nanoshell spectra have to be noted. First, transformation of doublet 83/100 cm^{-1} band into the single band at ~80 cm^{-1} is observed for the monomolecular shells. This doublet is associated with the complicated conformation of molecules and the existence of two isomeric states.[25] Therefore, this effect is in accordance with the notion about ''simplifying'' conformational state of the majority of PVP segments (flattened conformations, extending chains) in the adsorbed monolayers strongly interacting with a solid substrate.[15,16] Secondly, disappearance of the absorption band 245–247 cm^{-1} of torsional skeletal vibrations indicates some suppression of chain dynamics in PVP monolayers. Further, the far-IR spectra in the region of ~170-350 cm^1 directly characterize strong physical interactions at PVP-oxide interfaces (Table 2).

The spectra distinctly confirm arising and increasing the number of hydrogen bonds between NC = 0 groups of pyrrolidone rings and silanols of silica surface. The intensity of ~170 cm^{-1} band (k_{170}/k_{80} ratio) increases in the row: neat PVP–40PVP/60SiO_2– 20PVP/80SiO_2 compositions. At the same time, no essential hydrogen bonding at the PVP-alumina interfaces is registered (unchangeable k_{170}/k_{80} ratio). This result is in accordance with Figure 2.

Last but not least effect is arising of the pronounced additional absorption in the spectral range between ca. 250 and 350 cm^{-1} in the spectra of PVP nanoshells; it is estimated by the ratios of the absorption coefficients, k_{318}/k_{80}, k_{350}/k_{80}, and k_{350}/k_{444} (Figure 4, Table 2). Previously[14] we observed this effect for PVP/SiO_2 nanoparticles and supposed, tentatively, that it characterizes Lewis unterfacial interactions between strongly adsorbed segmental sequences (''trains'') and silica. It was supposed that the stronger L/B interfacial

Table 2.
Far-IR characterization of PVP-oxide interfacial interactions.[a)]

Sample interactions	Individual particle nanoshell thickness (nm)	Hydrogen bonding	PVP/oxide Lewis/Brønsted (~ 250 to 350 cm^{-1} region)		
		k_{170}/k_{80}	k_{318}/k_{80}	k_{350}/k_{80}	k_{350}/k_{444}
PVP		1.05	0.85	1.15	0.72
40PVP/60SiO_2	2	1.14	1.20	1.23	0.82
20PVP/80SiO_2	1	1.25	1.53	1.35	0.96
90PVP/10Al_2O_3	20	1.05	0.89	1.23	0.76
80PVP/20Al_2O_3	15	1.04	0.94	1.24	0.78
40PVP/60Al_2O_3	5	1.02	1.26	1.40	0.88
20PVP/80Al_2O_3	2	1.02	1.56	1.72	1.02

[a)]The coefficients k_{80} and k_{444} and their ratio remained practically unchangeable and were used as ''internal standards''.

Copyright © 2010 WILEY-VCH Verlag GmbH & Co. KGaA, Weinheim

interactions should be expected in the case of PVP adsorption onto metal oxide substrate including alumina. The data obtained herein testify in favor of such assignment. Thus, for the individual particles with monomolecular PVP nanoshells and $h_{PVP} = 2$ nm, k_{318}/k_{80}, k_{350}/k_{80} and k_{350}/k_{444} ratios are equal to 1.20, 1.23 and 0.82, respectively, in the case of silica core (40PVP/60SiO_2) but 1.56, 1.72 and 1.02 for the alumina core (20PVP/80Al_2O_3). Figure 4 and Table 2 also show that the impact of interfaces on the far-IR spectra becomes relatively slight at $h_{PVP} = 15$-20 nm (90PVP/10Al_2O_3 and 80PVP/20Al_2O_3 compositions).

Thus, if interfacial interactions between PVP and silica core are controlled by the hydrogen bonds and to some extent by LB-interactions, basically the latter control the PVP-alumina core interactions as it was supposed above.

Strong PVP/oxide interactions and peculiar conformational state of adsorbed polymer at interfaces have to affect the glass transition dynamics at interfaces. This is confirmed by the DSC experiments presented below.

Figure 5 shows the DSC curves (Perkin-Elmer DSC-2) characterizing PVP glass transition in waterless neat PVP and PVP/oxide samples. Glass transition temperature T_g at the half-height of heat capacity step, and the transition breadth $\Delta T_g = T_g'' - T_g'$ where T_g' and T_g'' are the temperatures of the glass transition onset and completion, respectively, are shown. DSC curves show a peculiar glass transition manifestation in

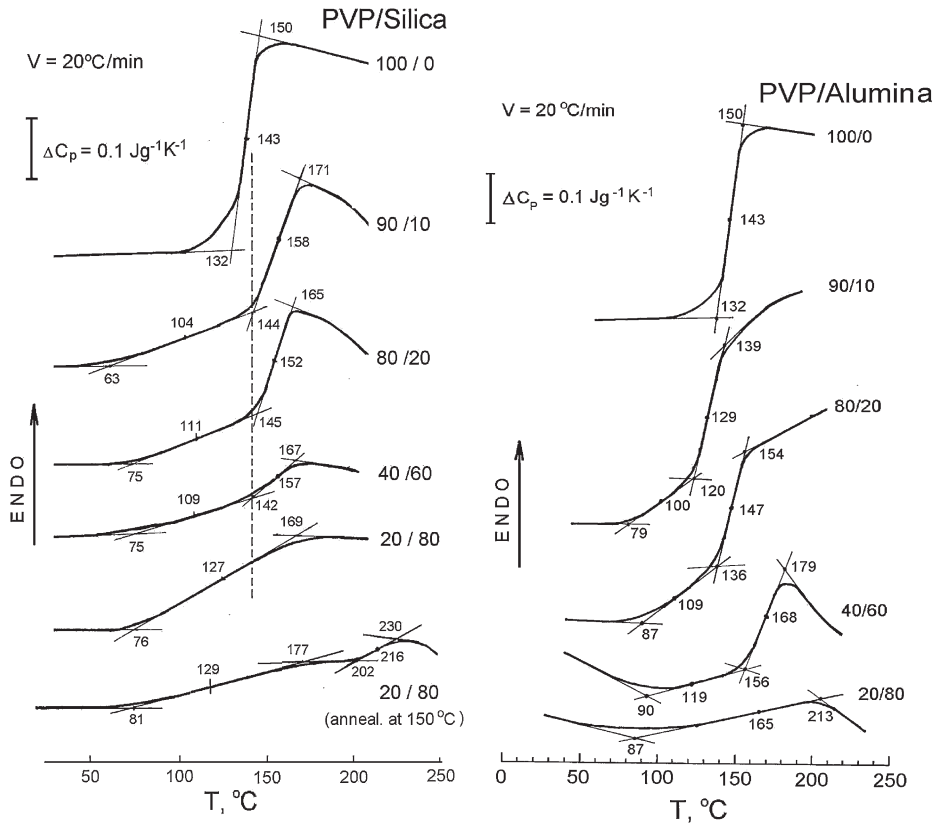

Figure 5.
DSC curves of neat PVP and the indicated PVP/oxide nanoparticles. The second scans were taken after heating samples to 217 °C with the rate $V = 20$ °C/min and subsequent cooling down to 20 °C with the rate $V = 320$ °C/min.

Copyright © 2010 WILEY-VCH Verlag GmbH & Co. KGaA, Weinheim

core-shell samples depending on their composition (shell thickness) and oxide type. No simple dependence of T_g on shell thickness but a strongly broadened in both directions (at the limit from 63 to 230 °C) and two-stage glass transition are observed for PVP shells, unlike the transition range $\Delta T_g = 18$ °C for neat PVP. Very broad one-stage transition is observed for monomolecular PVP shell at 20 wt% PVP in the core-shell particles.

Shell transition characteristics differed when using silica or alumina cores. The basic difference is the higher T_g' and T_g'' temperatures for the 20PVP/80Al_2O_3 and 40PVP/60Al_2O_3 particles. At the identical $h_{PVP} = 2$ nm (PVP monolayer) in the 40PVP/60SiO_2 and 20PVP/80Al_2O_3 particles, more strong LB interactions in the latter resulted in the higher T_g' and T_g'': 87 and 213 °C instead of 76 and 169 °C for the silica-containing particles (Figure 5).

As shown,[14] physical ageing, with arising of the endothermic peak after annealing, was suppressed for the monomolecular shell (20PVP/80SiO_2 particles) but the treatment at 150 °C resulted in arising new heat capacity step at 200–230 °C in the DSC curve (Figure 5).

Several dynamic modes contribute to the anomalously broad, complicated glass transition in PVP nanoshells. This was corroborated in the DSC experiments performed at different heating rates V, from 2.5 to 40 °C/min, and the determination of apparent activation energy Q values for segmental dynamics and their dispersions within the glass transition range using the formula:[26] $Q = -R\,\mathrm{d}\ln V/\mathrm{d}(T^{-1})$.

Figure 6 presents the Q dispersions within the glass transition of neat PVP and PVP in the nanoshells. The dashed line corresponds to Arrhenius relation (activation entropy $\Delta S = 0$) between Q and temperature for non-cooperative relaxations at frequency of $\sim 10^{-2}$ Hz. The departure of Q from this line characterizes in particular the degree of motional intermolecular cooperativity. Unlike ''normal'' cooperative dynamics in the narrow glass transition of neat PVP ($Q = 250$ kJ/mol, no

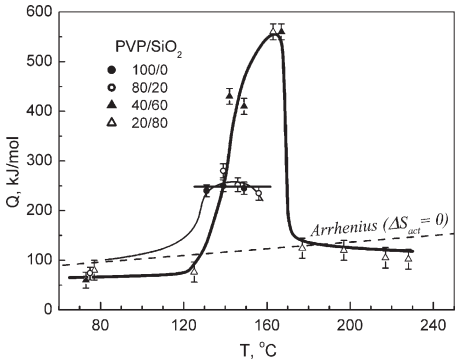

Figure 6.
Dispersions of apparent activation energies Q for segmental motion within waterless PVP glass transition as a function of temperature, as determined by DSC for neat PVP and three indicated core-shell compositions.

dynamic heterogeneity), dynamics in PVP shells sharply alters: the wide Q dispersions indicate the pronounced dynamic heterogeneity in the broad transition ranges, and $Q(T)$ plots are different for the shells with different thicknesses. Generally, they indicate two- or three dynamic modes within the glass transitions. At 80 wt% PVP, ''normal'' ($Q = 250$ kJ/mol) and ultra-fast Arrhenius ($Q = 75$ kJ/mol at 75 °C) relaxation modes are detected. Contrarily, ''normal'' glass transition dynamics, peculiar to bulk PVP, is absent at all in the glass transitions of the 40PVP/60SiO_2 and 20PVP/80SiO_2 samples with 2–5 and 1–2 nm thick shells, respectively. For the former sample three modes with $Q = 60$–70, 400 and 560 kJ/mol are registered.

The extraordinary dynamics is observed in a monomolecular shell of the 20PVP/80SiO_2 samples annealed at 150 °C. ''Abnormal'' (for glass transition) motions with the activation barriers, differing by an order of magnitude, are observed in this case: fast mode at 75–125 °C ($Q = 80$ kJ/mol) and two hindered dynamic modes, cooperative ($Q = 560$ kJ/mol, 160 °C) and Arrhenius-like ($Q \approx 100$ kJ/mol, 175–230 °C). Analysis of this multi-modal PVP dynamics at the interfaces was done[14] on the basis of the notions of constrained dynamics and nano-confinement effects. Strongly hindered

Copyright © 2010 WILEY-VCH Verlag GmbH & Co. KGaA, Weinheim

dynamics in PVP monolayers, cooperative at 160 °C or non-cooperative at 230 °C, may be related to extended segmental sequences ("trains") strongly attached to oxide surface via the LB and hydrogen bonding.

The opposite effect of arising a fast glass transition mode in the region of β - relaxation of PVP (at $\sim$ 60–80 °C), may be treated in terms of the common segmental nature of α - and β - relaxations in flexible-chain polymers (see reviews:[25-27]) this is due to collapse of motional cooperativity in loosely-packed nanovolumes and at free polymer surface.

Conclusion

3D silica- and alumina core-PVP shell nanoparticles with different shell thicknesses, down to monomolecular layer, were prepared using the pseudo-liquid state reactor and comprehensively characterized. The interfacial interactions and their contribution to nanoshell dynamics were studied. In recent work[14] and this paper for the first time far-IR spectroscopy and DSC analysis of the dispersion of activation barriers in the glass transition dynamics were applied to polymer nanolayers. The contributions of the strong hydrogen bonding and weak Lewis-Brønsted interactions to PVP/silica interfaces but only enhanced Lewis-Brønsted ones to PVP/alumina interfaces were revealed. For PVP monolayer, glass transition broadening and activation energy varying by an order of magnitude were shown; three ''abnormal'' dynamic modes constituted its glass transition, including constrained motions and ultrafast one caused by collapse of dynamic cooperativity. The distinct correlations between interfacial interactions and dynamics were found.

[1] C. L. Jackson, G. B. McKenna, *J. Non-Cryst. Solids* **1991**, *131–133*, 221.
[2] J. L. Keddie, R. A. L. Jones, R. A. Corey, *Europhys. Lett.* **1994**, *27*, 59.
[3] W. E. Wallace, J. H. van Zanten, W. L. Wu, *Phys. Rev. E* **1995**, *52*, R3329.
[4] J. A. Forrest, K. Dalnoki-Verres, J. R. Stevens, J. R. Dutcher, *Phys. Rev. Lett.* **1996**, *77*, 2002.
[5] E. P. Giannelis, R. Krishnamoorti, E. Manias, *Adv. Polym. Sci.* **1999**, *138*, 107.
[6] M. Alcoutlabi, G. B. McKenna, *J. Phys. Condens. Matter* **2005**, *17*, R461.
[7] J. A. Forrest, K. Dalnoki-Verres, *Adv. Colloid Interface Sci.* **2001**, *94*, 161.
[8] V. A. Bershtein, L. M. Egorova, P. N. Yakushev, P. Pissis, P. Sysel, L. Brozova, *J. Polym. Sci., Part B: Polym. Phys.* **2002**, *40*, 1056.
[9] V. Arrighi, I. J. McEwen, H. Qian, M. B. Serrano Prieto, *Polymer* **2003**, *44*, 6259.
[10] D. Fradiadakis, P. Pissis, L. Bokobza, *Polymer* **2005**, *46*, 6001.
[11] V. M. Gun'ko, E. F. Voronin, V. I. Zarko, E. V. Goncharuk, V. V. Turov *et al.*, *Colloids and Surfaces A* **2004**, *233*, 63.
[12] V. M. Gun'ko, E. F. Voronin, L. V. Nosach, E. M. Pakhlov, N. V. Guzenko *et al.*, *Adsorption Sci. Techn.* **2006**, *24*, 143.
[13] V. M. Gun'ko, E. F. Voronin, L. V. Nosach, E. M. Pakhlov, O. E. Voronina *et al.*, *Appl. Surf. Sci.* **2006**, *253*, 2801.
[14] V. A. Bershtein, V. M. Gun'ko, L. M. Egorova, N. V. Guzenko, E. M. Pakhlov, V. A. Ryzhov, V. I. Zarko, *Polymer* **2009**, *50*, 860.
[15] J. F. Douglas, H. M. Schneider, P. Franz, R. Lipman, S. Granick, *J. Phys. Condens. Matter* **1997**, *9*, 7699.
[16] R. L. Jones, S. K. Kumar, D. L. Ho, R. M. Breiber, T. P. Russel, *Macromolecules* **2001**, *34*, 559.
[17] M. Brogly, Y. Grohens, C. Labbe, J. Schultz, *Int. J. Adhes.* **1997**, *17*, 257.
[18] T. Hamieh, M. Rezzaki, J. Schultz, *J. Colloids Surf. A* **2001**, *189*, 279.
[19] M. Pattanaik, S. K. Bhaumik, *Mater. Lett.* **2000**, *44*, 352.
[20] C. F. Huang, S. W. Kuo, F. J. Li, C. F. Wang, C. J. Hung, F. C. Chang, *Polymer.* **2006**, *47*, 2060.
[21] B. A. Morrow, I. A. Cody, *J. Phys. Chem.* **1976**, *80*, 1995.
[22] K. Tanabe, *Solid Acids and Bases*, Kodansha, Tokyo 1970.
[23] T. L. Lebedeva, M. M. Fel'dshtein, S. A. Kuptsov, N. A. Platé, *Polym. Sci. A* **2000**, *42*, 989.
[24] V. M. Gun'ko, V. V. Turov, P. P. Gorbic, *Water at Interfaces*, Naukova Dumka, Kiev 2009 (in Russian).
[25] V. A. Bershtein, V. A. Ryzhov, *Adv. Polym. Sci.* **1994**, *114*, 43.
[26] V. A. Bershtein, V. M. Egorov, ''*Differential Scanning Calorimetry of Polymers. Physics, Chemistry, Analysis, Technology*'', Ellis Horwood, New York 1994.
[27] V. A. Bershtein, V. M. Egorov, L. M. Egorova, V. A. Ryzhov, *Thermochim. Acta* **1994**, *238*, 41.

Copyright © 2010 WILEY-VCH Verlag GmbH & Co. KGaA, Weinheim